

Determination of the Structure and Density of Melts at High Pressures and High Temperatures

G. Shen,¹ N. Sata,¹ M. Newville,¹ M. L. Rivers,^{1,2} S. R. Sutton^{1,2}

¹Consortium for Advanced Radiation Sources and ²Department of Geophysical Sciences, University of Chicago, Chicago, IL, U.S.A.

Introduction

The observation [1] of diffuse scattering in a diamond anvil cell (DAC) offers possibilities of structure studies of melts at high pressures and high temperatures. The number of studies on the structure of melts under high pressure, particularly with the use of synchrotron radiation, is growing [2-5]. These studies are limited to applications of large-volume presses and therefore cover a limited pressure range. In this study, we demonstrate the feasibility of determining the structures of melts in a DAC.

Methods and Materials

An externally heated DAC (DXR-7, Diacell) was used in this study. The main feature of the DAC design is the use of four cartridge heaters inserted in the cell body, which provide heat to the whole cell and result in a uniform temperature distribution inside the cell. A rhenium gasket was pre-indented to about 50 μm in thickness with diamond anvils of 500 μm in culet diameter. Two holes 100 μm in diameter were drilled at the positions equidistant from the center. Indium powder (99.999%, Alfa Aesar) was loaded into one hole. The other hole was loaded with NaCl. A NaCl chip ($\sim 5 \mu\text{m}$) was put at the corner of the chamber with indium for the pressure measurement.

The x-ray diffraction experiment was performed at the GeoSoilEnviro Consortium for Advanced Radiation Sources (GSECARS) beamline 13-ID-D at APS. A charge-coupled device (CCD) detector (MAR-CCD) was used to collect diffraction patterns. The monochromatic x-ray beam was produced by using a channel-cut crystal (silicon 220) and was fixed at an energy of 29.200 keV, calibrated by scanning through the tin metal K-absorption edge. The x-ray beam size was controlled by a slit system to $150 \times 150 \mu\text{m}$ and then focused to a beam size of $5 \mu\text{m}$ (vertical) $\times 5 \mu\text{m}$ (horizontal) at full width at half maximum (FWHM) by Kirkpatrick-Baez mirrors [6]. Typical CCD exposure times were 60 s.

The x-ray intensity before and after the DAC was monitored by an ion chamber and a photodiode, respectively. The photodiode reading reflects the x-ray absorption of the sample and the DAC, while the reading from the ion chamber is used for normalization.

Results and Discussion

Density of Melts

A standard was introduced in the sample preparation for measuring the density of molten indium. From the known density of the standard material determined by x-ray diffraction, the thickness of the sample chamber can be obtained. The sample configuration and one typical x-ray transmission scan is given in Fig. 1 with the monochromatic beam of 29.200 keV. According to the absorption law, $I = I_0 \exp(-\mu \rho l)$, where I = the transmission intensity, I_0 = the normalized incident intensity, μ = the mass absorption coefficient, ρ = the density of the sample, and l = the thickness of the sample. The thickness l can be obtained by:

$$l = \ln(I_{\text{NaCl}}/I_{\text{Re}}) / (\mu_{\text{Re}} \rho_{\text{Re}} - \mu_{\text{NaCl}} \rho_{\text{NaCl}}). \quad (1)$$

The quantities on the right side of Eq. (1) are either known values (μ) or measurable (ρ and l). The x-ray transmission can be directly measured, as shown in Fig. 1. The mass

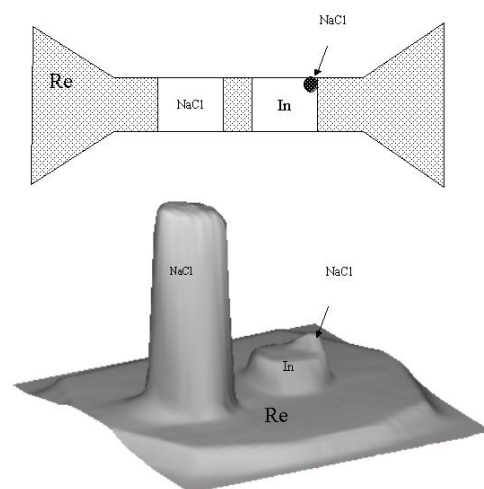


FIG. 1. Top: A dual-hole configuration of the rhenium gasket between two diamond anvils. Bottom: An x-ray transmission profile measured by a photodiode with a monochromatic x-ray beam at 29.200 keV. The profile was obtained by scanning the sample position in a step of $5 \mu\text{m}$ with an x-ray beam size of $5 \times 5 \mu\text{m}$ at the FWHM.

absorption coefficient at 29.200 keV is obtained from a report by the National Bureau of Standards. The densities of NaCl and rhenium are obtained by x-ray diffraction, since these two materials were in crystalline states in the pressure/temperature range of this study. By assuming the same thickness across the sample and the standard, we obtain the density of the molten state:

$$\rho_{\text{In}} = [\ln(\mathbf{I}_{\text{NaCl}}/\mathbf{I}_{\text{In}}) + \mu_{\text{NaCl}}\rho_{\text{NaCl}}]/\rho_{\text{In}}. \quad (2)$$

Note that the distance between two diamond anvils is not always the same across the culet area. Especially at pressures over 30 GPa, deformation occurs with diamond anvils [7], resulting in a variable thickness profile. In this case, a 2-D scan is required for obtaining a thickness profile across the whole culet area.

The transmission data shown in Fig. 1 were measured under conditions (3.4 GPa and 448K) in which the indium was at crystalline state. By measuring its x-ray diffraction, we obtained a density of $7.667 \pm 0.016 \text{ g/cm}^3$ for the crystalline indium. By the absorption measurement and by employing Eqs. (1) and (2), we obtained a thickness of $51.39 \pm 0.22 \text{ }\mu\text{m}$ and a density of $7.72 \pm 0.11 \text{ g/cm}^3$, where the standard errors were estimated by the errors in the x-ray transmission intensities and in the molar volumes by diffraction. The relative error $\Delta\rho/\rho$ by the absorption method is 1.4% compared to 0.2% by diffraction. The density difference between the two methods is 0.053 g/cm^3 , which is within the standard error of 0.11 g/cm^3 by the absorption method. We found that the main source of error for the absorption method is the transmission intensities.

We performed an isothermal compression at $710 \pm 3\text{K}$. The compression behavior of molten indium is given in Fig. 2. The line is the fit with Birch-Murnaghan equation of state, with parameters of $\rho_0 = 6.81 \text{ g/cm}^3$, $K_0 = 23.2 \pm 0.6 \text{ GPa}$, and $K' = 4$. From the compression data [8] at 300K for crystalline indium, the Birch-Murnaghan equation state parameters are $\rho_0 = 7.310 \text{ g/cm}^3$, $K_0 = 45.7 \pm 0.6 \text{ GPa}$, and $K' = 5.2 \pm 0.2 \text{ GPa}$. Clearly, the melt is more compressible than that of the corresponding solid.

Structure of Melts

The observed x-ray scattering intensity $\mathbf{I}^{\text{obs}}(Q)$ may be expressed by:

$$\mathbf{I}^{\text{obs}}(Q) = PA[\mathbf{I}^{\text{coh}}(Q) + \mathbf{I}^{\text{inc}}(Q) + \mathbf{I}^{\text{mul}}(Q) + \mathbf{I}^{\text{back}}(Q)], \quad (3)$$

where $Q = 4\pi\sin(\theta)/\lambda$; P = the polarization factor; A = the absorption factor; \mathbf{I}^{coh} , \mathbf{I}^{inc} , and \mathbf{I}^{mul} = the coherent, incoherent, and multiple scattering intensities, respectively; and \mathbf{I}^{back} = the background scattering intensity from surrounding materials (diamond anvils in this case). \mathbf{I}^{mul} is relatively weak and is usually neglected in x-ray

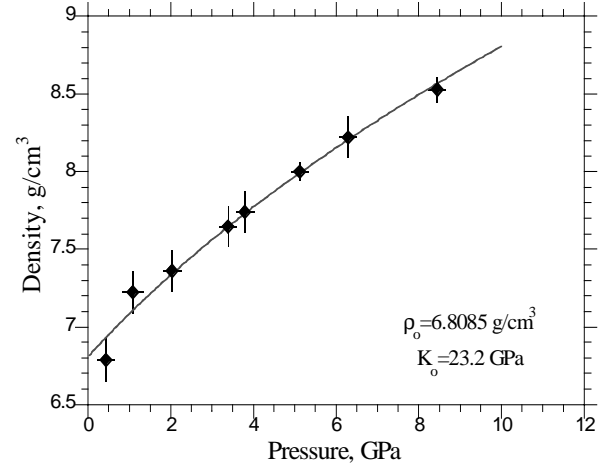


FIG. 2. Densities of molten indium at 710(3)K at high pressures. The line is the fit with the second-order Birch-Murnaghan equation of state with the parameters shown in the figure.

scattering [9, 10]. \mathbf{I}^{coh} can be expressed as $f_a^2 S(Q)$, where f_a = the atomic scattering factor and $S(Q)$ = the structure factor. To obtain $S(Q)$, \mathbf{I}^{inc} and \mathbf{I}^{back} have to be subtracted from $\mathbf{I}^{\text{obs}}(Q)$.

The diffraction intensity was then converted into the structure factor, $S(Q) = N\mathbf{I}^{\text{coh}}(Q)/f_a^2(Q)$. Here N = the normalization factor for $S(Q) \rightarrow 1$ at $Q \rightarrow \infty$. Figure 3 shows the structure factors measured at various pressures at a temperature of 710(3)K. From $S(Q)$, the pair distribution function $g(r)$ is given by Fourier transformation of $Q_i(Q) = Q[S(Q) - 1]$. The density data measured in this study were used in the calculation of $g(r)$.

The pair distribution function $g(r)$ of molten indium shows a sharp first peak at about 3.0 Å and a broad second peak at around 6.5 Å. There are some spurious ripples at both sides of the first peak, which result from the limited range of Q over which $S(Q)$ was measured and from errors in $S(Q)$ itself. With increasing pressures, the first peak of $g(r)$ becomes sharper and more intense, indicating that the atoms are more localized around the nearest neighbor. This effect is also noticeable in $S(Q)$ (Fig. 3), where the intensity of the first peak at around Q of 2.3 \AA^{-1} increases with pressure. With the concept of the coordination number (CN) at the nearest neighbor, this phenomenon can be described in a quantitative way. CN was calculated by the integration of the first peak in the radial distribution function: $\text{RDF} = 4\pi r^2 g(r)$. The result (Fig. 4) shows that CN increases with pressure almost linearly within experimental errors.

Acknowledgments

This work is supported by the National Science Foundation (NSF) Division of Earth Sciences EAR 00011498. GSECARS is supported by the NSF Earth

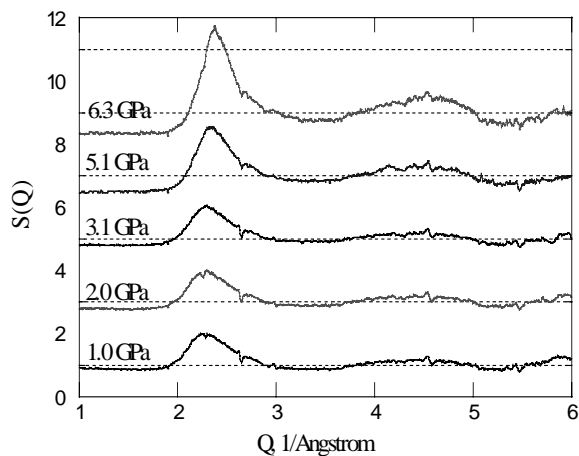


FIG. 3. Structure factors of molten indium as a function of pressure at a temperature of 710(3)K. It can be seen that intensities of the first peak increase with increasing pressure.

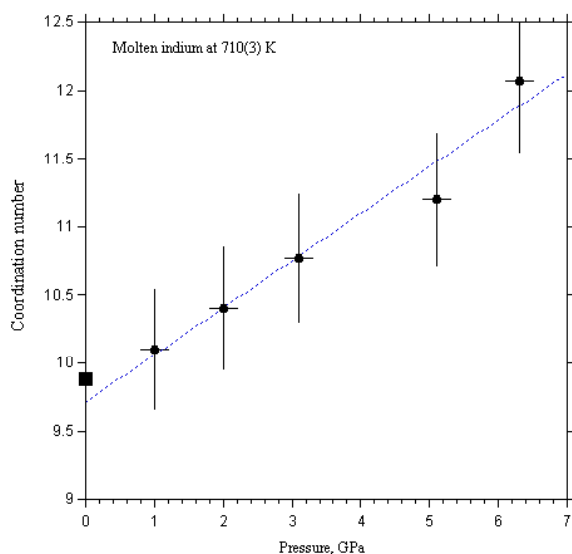


FIG. 4. The coordination number of the nearest neighbor of molten indium as a function of pressure at 710(3)K. The error bars are at the $\pm 5\%$ level, a number estimated from the uncertainties in the choice of the limits at both sides of the first peak in $g(r)$ and errors in $g(r)$ itself. Uncertainties arising from the errors in density are less than 2%.

Science Instrumentation and Facilities Program and U.S. Department of Energy (DOE) Geoscience Program. Use of the APS was supported by the DOE Office of Science, Office of Basic Energy Sciences, under Contract No. W-31-109-ENG-38.

References

- [1] G. Shen, N. Sata, M. L. Rivers, and S. R. Sutton, *Appl. Phys. Lett.* **78**, 3208-3210 (2001).
- [2] S. Urakawa, N. Igawa, O. Shimomura, and H. Ohno, *Am. Mineral.* **84**, 341-344 (1999).
- [3] Y. Katayama, T. Mizutani, W. Utsumi, O. Shimomura, and K. Tsuji, *Physica Status Solidi B: Basic Research* **223**, 401-404 (2001).
- [4] C. Sanloup, F. Guyot, P. Gillet, G. Fiquet, R. J. Hemley, M. Mezouar, and I. Martinez, *Europhysics Lett.* **52**, 151-157 (2000).
- [5] J. Y. Raty, J. P. Gaspard, T. Le Bihan, M. Mezouar, and M. Bionducci, *J. Phys. Condens. Matter* **11**, 10243-10249 (1999).
- [6] P. Eng, M. L. Rivers, B. X. Yang, and W. Schildkamp, *Proc. SPIE* **2516**, 41-51 (1995).
- [7] R. J. Hemley, H. K. Mao, G. Shen, J. Badro, P. Gillet, M. Hanfland, and D. Häusermann, *Science* **276**, 1242 (1997).
- [8] R. W. Vaughan and H. G. Drickamer, *J. Phys. Chem. Solids* **26**, 1549-1553 (1965).
- [9] N. E. Cusack, *The Physics of Structurally Disordered Matter: An Introduction* (IOP Publishing Ltd., Adam Hilger, Bristol and Philadelphia, PA, 1987).
- [10] Y. Waseda, *The Structure of Non-crystalline Materials* (McGraw-Hill Inc., 1980).